Report No. BMI-1314
C-83 - Reactors - Special Features
of Military Package
Power Reactors
(M-3679, 22nd Ed.)

Contract No. W-7405-eng-92

NEUTRON-FLUX MEASUREMENTS IN A CONCENTRIC-CYLINDER FUEL ELEMENT

by

James N. Anno
Barry P. Fairand
Joel W. Chastain, Jr.

January 29, 1959

BATTELLE MEMORIAL INSTITUTE
505 King Avenue
Columbus 1, Ohio

DISCLAIMER

TABLE OF CONTENTS

	Page
ABSTRACT	5
INTRODUCTION	5
DESCRIPTION OF FACILITIES AND FUEL SPECIMEN	6
Battelle Research Reactor, In-Pile Loop, and Loop Mock-Up	6
Description of the Mark II Element	6
EXPERIMENTAL PROCEDURES	9
Absolute Flux Measurements	10
FLUX DETERMINATIONS	11
Unperturbed Flux Distributions at the Core Face	11
Radial and Vertical Flux Distributions	11
Peripheral Flux Distribution	17
POWER PREDICTED FROM FLUX MEASUREMENTS	17
Power Generated by Epicadmium Neutrons	20
DISCUSSION OF ERRORS	20
COMPARISON OF FLUX-DETERMINED POWER WITH HEAT-BALANCE POWER	21
SUMMARY AND CONCLUSIONS	22
REFERENCES	24

NEUTRON-FLUX MEASUREMENTS IN A CONCENTRIC-CYLINDER FUEL ELEMENT

James N. Anno, Barry P. Fairand, and Joel W. Chastain, Jr.

In research in support of the GCRE, neutron-flux measurements in a concentric-cylinder fuel element were made in a gas-cooled in-pile loop operated adjacent to the core of the BRR. The fuel element comprised four concentric fuel cylinders. Each fuel annulus (outside diameters: 1.248, 1.018, 0.810, and 0.590 in.) consisted of a 0.031-in.-thick core of UO_2 dispersed in Type 347 stainless steel and clad on each side with 0.007 in. of Type 318 stainless steel. The element was 24 in. long and the total uranium-235 content was approximately 192 g.

Radial, vertical and peripheral flux distributions were studied. The vertical flux profile was cosine-shaped with a peak-to-average ratio of 1.26. The peripheral variation around the loop wall could also be fitted to a cosine curve (with a peak-to-average ratio of 1.10). The average radial flux depression from the outer fuel cylinder to the center of the element was a factor of 2.14.

Power generation in the element calculated from flux measurements agreed to within 10 per cent with the power generated by measuring gas flow rate and temperature rise across the fuel element. The ratio of peak-to-average power density was found to be 1.75.

INTRODUCTION

As part of the materials research program for the Gas-Cooled Reactor Experiment (GCRE), an in-pile gas-cooled loop has been installed at the Battelle Research Reactor.[1] This loop has been operating since March, 1958, and has been used to test both flat-plate and concentric-cylinder fuel elements. Neutron-flux measurements were made in each fuel element prior to its operation in the loop. Flux measurements with the flat-plate fuel element (designated as Mark I for reference purposes) have been reported previously.[2] This report presents measurements made with a concentric-cylinder element (Mark II) and includes axial, radial, and peripheral flux distributions.

The objective of the flux measurements was (1) to predict the distribution of power generation (fissioning), and (2) to predict the total power of the loop. From an engineering standpoint, the distribution of power is frequently the more important because of its relation to the detailed temperature and stress distributions. Also, the total power of the loop can be measured by over-all heat-balance methods more accurately than by absolute flux-measurement techniques.

(1) References at end.

DESCRIPTION OF FACILITIES AND FUEL SPECIMEN

Battelle Research Reactor, In-Pile Loop, and Loop Mock-Up

The Battelle Research Reactor (BRR) is a modified pool type operating at 1-megawatt power.[3] The core is composed of MTR-type fuel elements suspended from a bridge into a large pool of water. Normally the reactor is operated at one end of the pool where the pool walls are modified to form a stall area. In this location six beam tubes and a thermal column partially cover three faces of the core. The fourth (open) face of the core is used for large experiments which are suspended in the pool.

The loop is a high-pressure gas recirculating loop with the entire circulating system submerged in the reactor pool.[1] The test element is vertical when in position in the loop and the center line of the fuel element is near the center line of the reactor fuel. The entire loop is suspended from a second, movable bridge which is independent of the core bridge. With this arrangement the loop can be moved away from the core face for maintenance. During operation the front of the loop is about 1/8 in. from the core face. Even with this proximity the interaction between the core and loop is small, as evident from the small reactivity contribution of the loop (less than 0.001 Δk).

The core loading used during loop operation and the location of the loop relative to the core are shown in Figure 1. The core contains 31 fuel elements, with the loop located in a pocket formed by the core face and two of the elements. The nearest reactor control rod is separated from the loop by a single row of fuel elements. This rod is used as a safety rod and is always withdrawn from the core during operation.

For the flux measurements, a special mock-up of the loop was constructed which duplicates the loop in the vicinity of the reactor core both in dimensions and materials.[2] Before operating a new fuel element in the loop, detailed flux measurements are made with the element in the mockup.* Measurements of the neutron flux in both the loop and mock-up verify that the two are identical nuclearwise.

Description of the Mark II Element

The Mark II element is composed of four concentric fuel cylinders surrounded by an insulating jacket. A sketch of the element cross section is shown in Figure 2. Each cylinder consists of three 120-deg segments held together by special clips. The fuel plates are supported by the arms of a spider welded to a central column support. The insulating jacket is a stainless steel-Thermoflex-stainless steel sandwich.

Each fuel cylinder is 0.045 in. thick (including cladding), contains highly enriched uranium in the form of 25 w/o UO_2 dispersed in a Type 347 stainless steel core matrix, and is clad with 0.007-in. Type 318 stainless steel. The fuel-bearing length

*On occasions when the loop was available, the flux measurements were made in the actual loop.

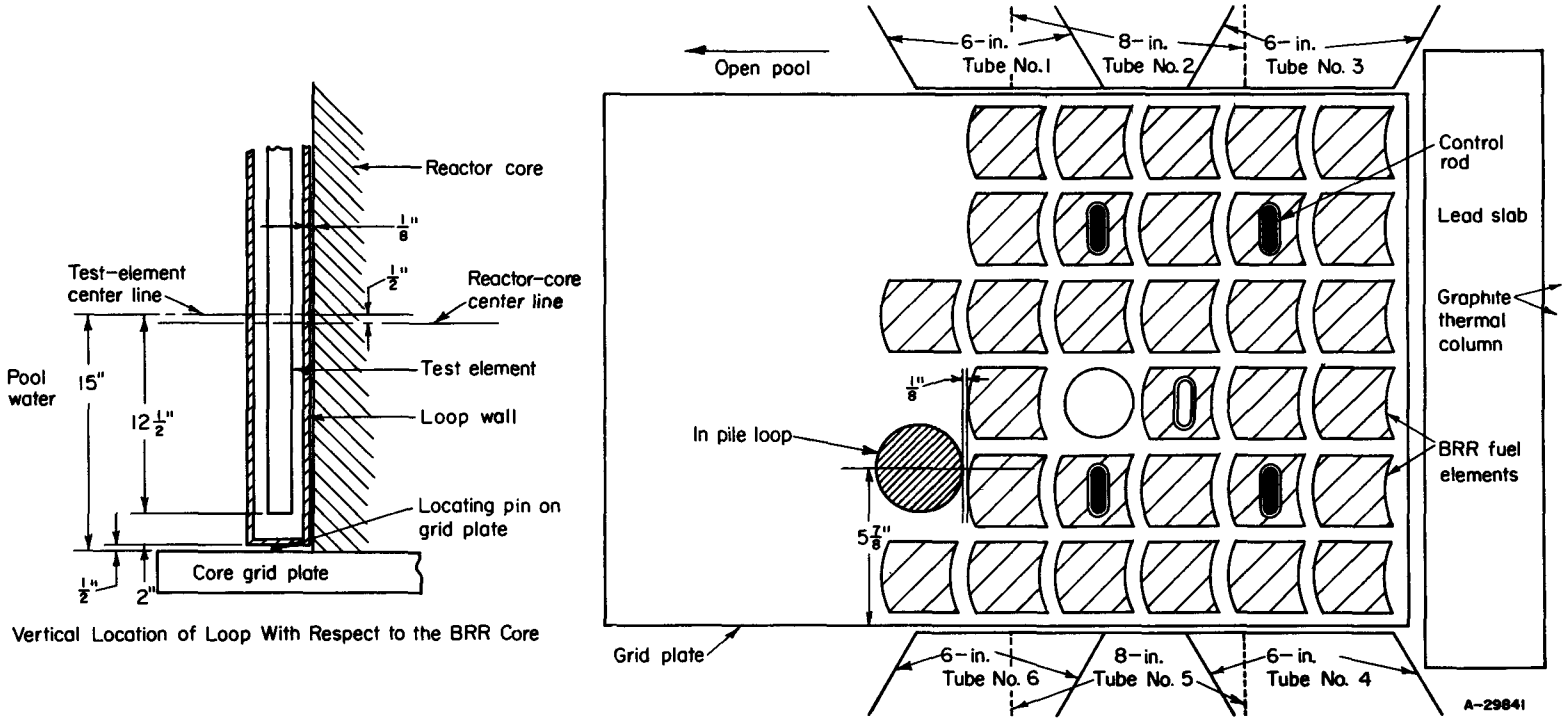

FIGURE 1. GENERAL ARRANGEMENT OF LOOP AND REACTOR CORE

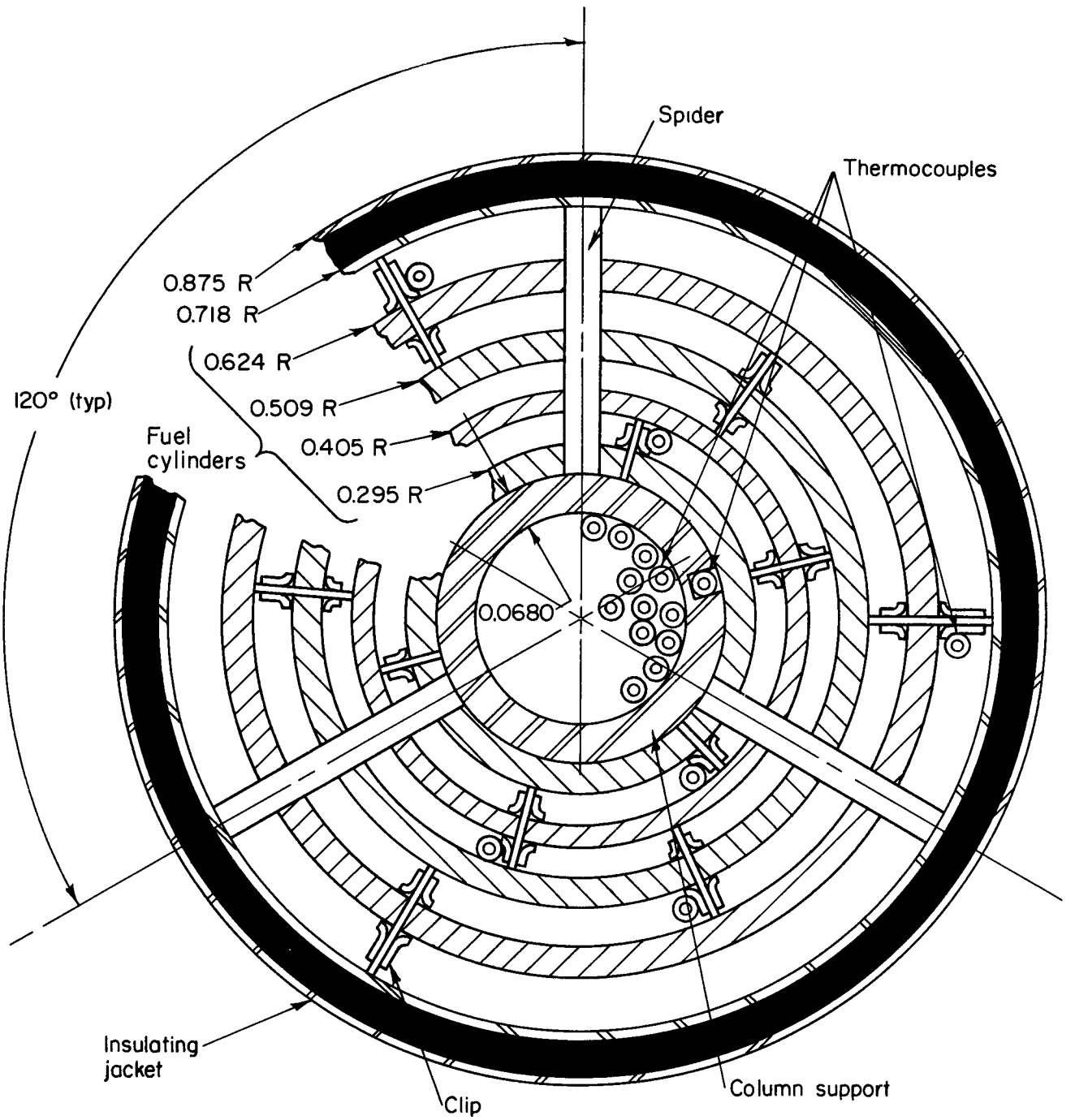

FIGURE 2. SKETCH OF MARK II FUEL SPECIMEN

of each cylinder is 24 in. (closely matching the fuel length in the Battelle Reactor core). The uranium-235 content of each cylinder is given in Table 1.

TABLE 1. FUEL CONTENT OF CYLINDERS IN MARK II ELEMENT

Cylinder	Inside Diameter, in.	Uranium-235 Content, g
1	0.500	26.72
2	0.720	41.12
3	0.928	54.38
4	1.158	70.13
	Total	192.35

EXPERIMENTAL PROCEDURES

The neutron fluxes were mapped by the activation technique. Manganese-iron wires (0.033 in. in diameter by 28 in. long) containing approximately 15 w/o manganese were activated to obtain flux distributions in the test specimen. Absolute flux measurements were made by activating gold foils 0.001 in. thick by 1/2 in. in diameter. Cadmium ratios were determined with 0.015-in.-thick cadmium sleeves for the manganese-iron wires and 0.020-in.-thick cadmium covers for the gold foils.

The wires were positioned in the fuel element by special jigs attached to the ends of the element. Gold foils were attached with Mylar tape. The element was then inserted into either the loop or loop mock-up and irradiated at low reactor power (400 to 1000 w). Low-power irradiation was sufficient to obtain the desired activity in the wires and foils and minimized the induced radioactivity in the test element. The low induced radioactivity in the element permitted direct access to it to remove the foils and wires for counting after a decay period of only a few hours.

The linearity of the ionization chamber, monitoring reactor power, was checked several times during the program by comparing it with a fission chamber to assure that no significant errors were introduced by extrapolating the flux data to full reactor power. In general, indicated power was corrected by about 10 per cent to account for instrument response to residual core gamma rays. Also, activations were corrected for irradiation during reactor startup and shutdown.

After irradiation the wires were cut into 1-in. lengths and the activity of each length was counted. The counting equipment included three photomultiplier channels,

two of which had print-out devices which automatically printed the total counts shown on the scaler of each circuit at the end of a counting period. The third channel operated control circuits at the end of a preset count and was used for timing the other two counting channels. This procedure automatically compensates for decay time of the activated wire. A sample changer moved the wire segments from a storage hopper to a position under the first counter. Each piece was counted and moved automatically to a second counter where it was counted a second time; the wire was then moved to a storage hopper. The data from the two channels were compared to detect spurious counts or inconsistencies. When good agreement was indicated, the data from the two channels were averaged to obtain the activity of each wire.

Absolute Flux Measurements

Since the manganese-iron wire activities were used to obtain relative flux distributions, absolute counting was not required. However, to obtain the neutron flux from the gold-foil activities the absolute activity was determined. Activity measurements were made with a scintillation spectrometer equipped with a 1-3/4 by 2-in. Harshaw sodium iodide thallium-activated crystal and a DuMont Type 6929 photomultiplier tube.

The thermal-neutron flux was obtained from the gold-foil activity by the relation

$$\phi = \frac{C_p \left(1 - \frac{1}{CR}\right)}{\Sigma_{act} M_g (1 - e^{-\lambda T})(e^{-\lambda t})\, E_{pp}}, \qquad (1)$$

where

ϕ = thermal-neutron flux, $n/(cm^2)(sec)$

C_p = count rate at the photopeak of gold-198 (corrected for background), counts per sec

CR = cadmium ratio

Σ_{act} = macroscopic thermal activation cross section for gold, cm^2 per g

M_g = mass of gold foil, g

λ = decay constant of gold-198, sec

T = duration of foil irradiation, sec

t = time after irradiation ended that C_p was observed, sec

E_{pp} = photopeak efficiency of counter.

The photopeak efficiency was determined by calibrating the counter with a standard cesium-137 source in the form of a 1/2-in.-diameter disk to match the foil geometry, using the known relationship between photo efficiency and gamma-ray energy for the crystal. Backscattering of gammas was reduced by suspending the scintillation head from the ceiling of the counting room in a Lucite sample holder.

FLUX DETERMINATIONS

Unperturbed Flux Distributions at the Core Face

The unperturbed neutron-flux distribution was measured in the pool water adjacent to the core face in the normal vicinity of the loop. The flux was mapped in the pocket formed by the fuel elements protruding from the core (see Figure 1) in a volume 24 by 5 by 6 in. Thirty-six manganese-iron wires, each 24 in. long, and spaced as shown in Figure 3, were suspended between two plastic plates supported on the corners by aluminum rods. The wires were positioned vertically to match approximately the location of the test element during loop operation. After irradiation the activated wires were cut into 1-in. segments and counted.

To show the gross unperturbed flux variation in the horizontal plane, the relative flux averaged over each wire is given below the wire location in Figure 3. As seen from this diagram, in a plane parallel with the core face the flux peaks near Position 54 and then decreases gradually toward Position 51. The average behavior of the flux perpendicular to the core face is shown graphically in this same figure. The characteristic reflector flux peak is observed 3/4 to 1 in. from the core face. A short distance beyond the peak the flux attenuates with a relaxation length of about 6 cm, which is characteristic of thermal-neutron attenuation near the core.(4) The vertical flux variation (not shown) is roughly a cosine distribution with a peak-to-average flux ratio of 1.33.

Since the data indicate a fairly gradual change in the flux distribution in this region, accurate positioning of the loop is not critical. This fact greatly expedites positioning the loop at the start of each reactor operating cycle.

Radial and Vertical Flux Distributions

The first series of flux measurements in the concentric-cylinder fuel element consisted of radial and vertical plots, obtained by activating six manganese-iron wires located along a particular radius. The arrangement of the wires in the fuel element and their relation with respect to the reactor core are shown in Figure 4. Corrections to the wire activities due to variation of the cadmium ratio along the radius were small and to a good approximation the wire activity is a direct indication of the thermal-neutron flux.

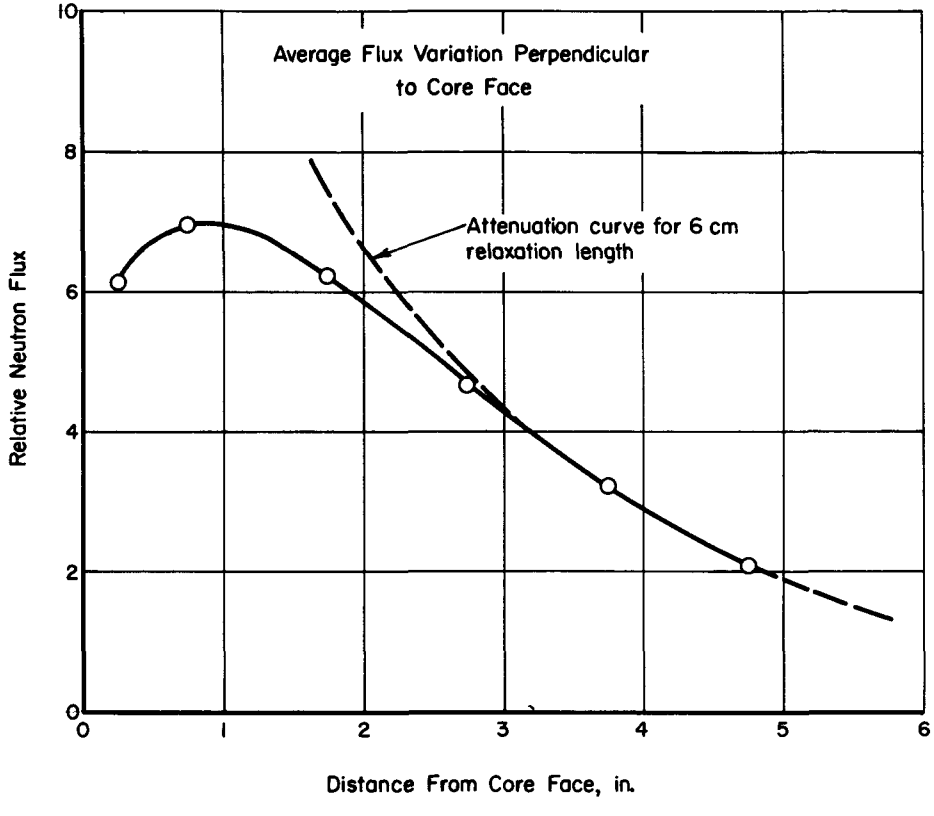

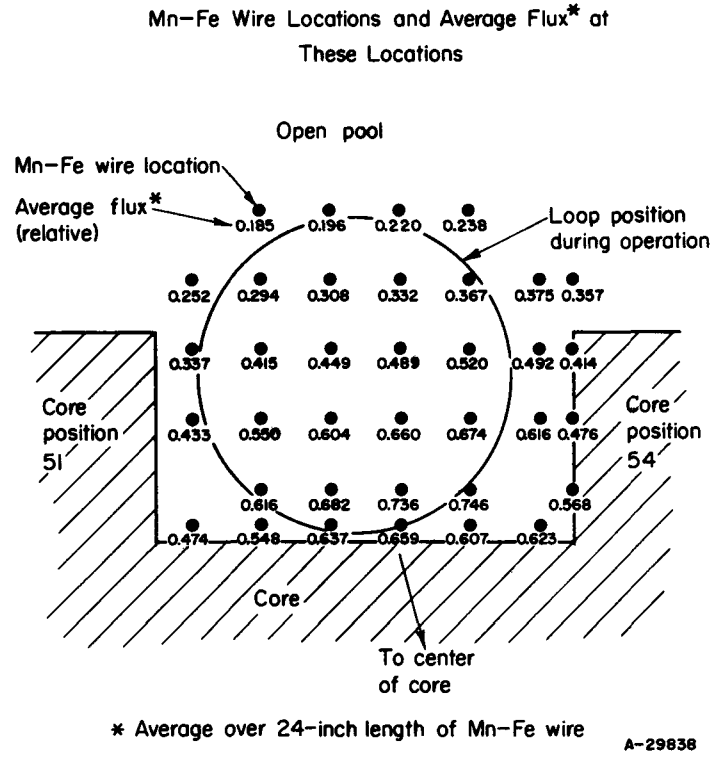

FIGURE 3. UNPERTURBED FLUX DISTRIBUTION IN VICINITY OF LOOP

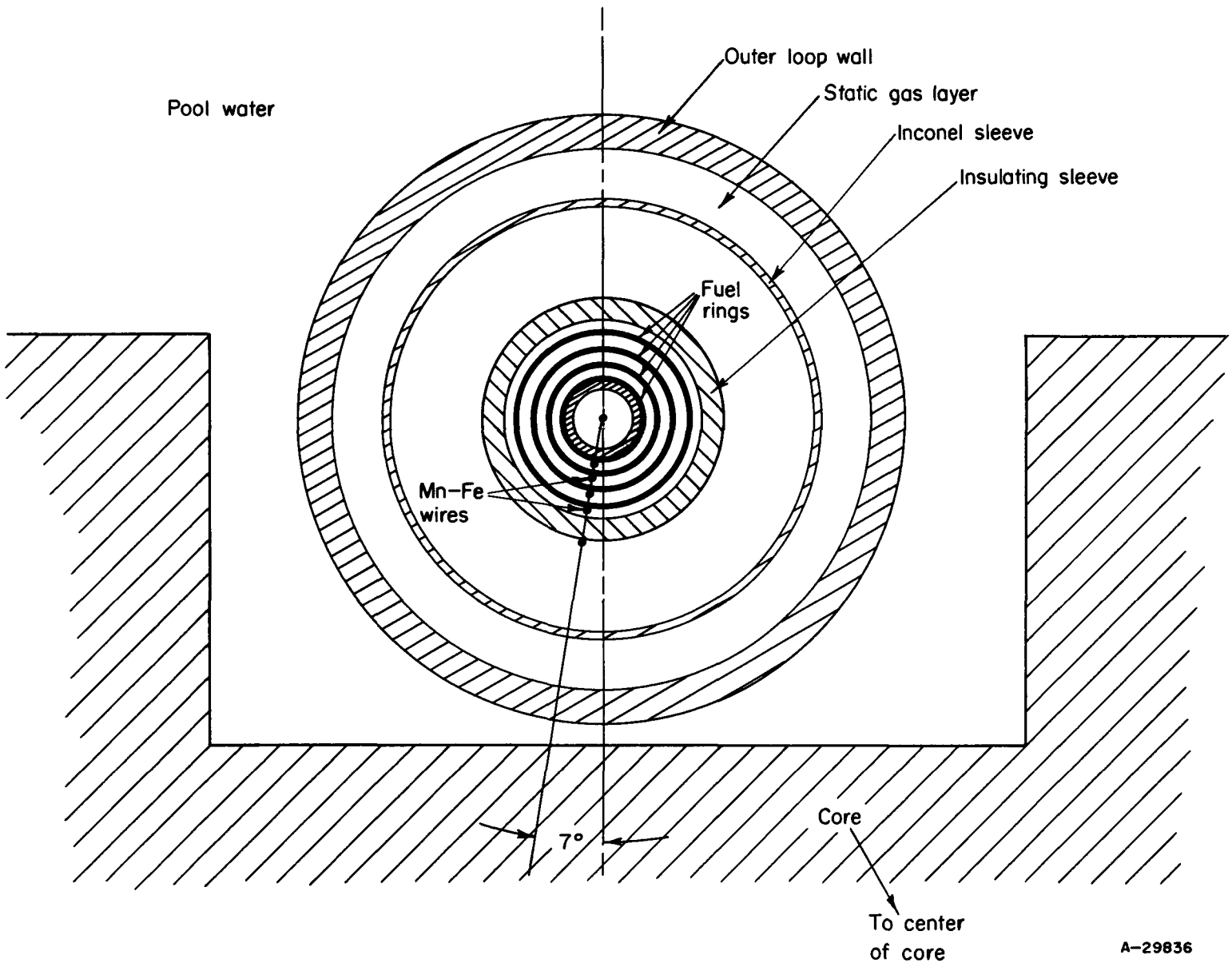

FIGURE 4. LOCATION OF MANGANESE-IRON WIRES FOR MAPPING RADIAL AND VERTICAL FLUX DISTRIBUTIONS

The average radial flux behavior obtained by averaging the radial plots along each 1-in. vertical section of the element is shown graphically in Figure 5. The curve drawn through the data points assumes that the principal flux drop occurs across the fuel plate with very little drop across the gas coolant channel. Data from the critical-assembly experiments with similar fuel elements support this assumption. It was found that the flux decreased from the surface of the outer fuel cylinder to the center of the element by a factor of 2.20 ± 0.03 standard deviation. The small deviation from the average indicates that the radial flux behavior is approximately independent of vertical location in the element. A much smaller flux drop, approximately a factor of 1.12, occurs across the insulating sleeve.

The vertical flux profile was also obtained from these six manganese-iron wires. The corrections to the wire activities for axial variation of the cadmium ratio were negligible and hence the profiles are thermal-neutron flux distributions. As mentioned previously, it was found that the vertical flux profile was approximately independent of radial location. Wires activated around the periphery of the fuel element showed that the vertical distribution was also insensitive to peripheral (angular) position. The magnitude of the flux is, of course, strongly dependent on radial location and to a lesser extent on peripheral location. The average vertical behavior of the flux is shown graphically in Figure 6.

The vertical flux distribution has approximately a cosine behavior with the peak flux occurring about 13 in. from the top of the fuel region (approximately 1 in. below the fuel center line). At the lower end of the test element a small flux peak is observed. This peak is apparently due to neutron reflection from the water and aluminum 2 in. below the element (see Figure 1). At the upper end of the fuel element no peak is observed since the gas-filled loop piping extends several feet above the element. As seen from the graph the vertical variation of the flux is not severe; the vertical peak-to-average flux ratio is only 1.26.

Superimposed on the graph of the test element data is the vertical flux profile for the center of the reactor fuel element immediately in front of the loop. It should be noted that the core flux peaks below the fuel center line and this fact, in addition to the relative axial location of loop and reactor core, is responsible for the slight asymmetry of the vertical flux profile about the center line of the test element. A damping effect of the vertical flux variation from core to loop is also apparent. The vertical peak-to-average flux ratio in the core fuel element is 1.40 compared with 1.26 for the test element in the loop. Since the unperturbed flux measurements in the pool water at the location normally occupied by the loop indicated a peak-to-average ratio of 1.33, it may be assumed that about one-half of this damping is due to geometrical effects. It is possible that the other half of the damping effect is due to axial neutron streaming in the loop. This speculation is supported by data from experiments with the GCRE critical assembly[5] in which the axial flux distribution with the core flooded was compared with the distribution with the core not flooded.

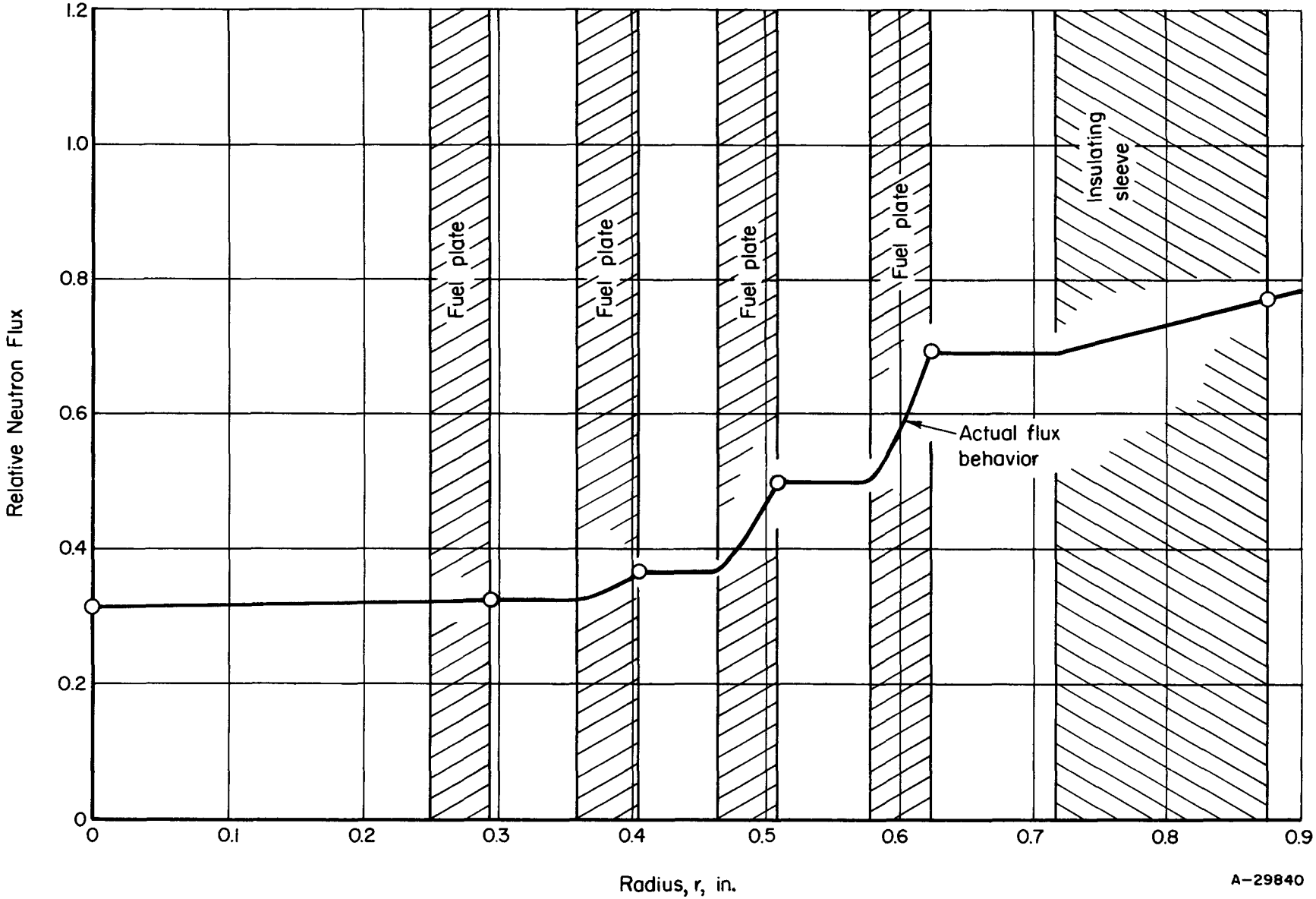

FIGURE 5. RADIAL FLUX DISTRIBUTION

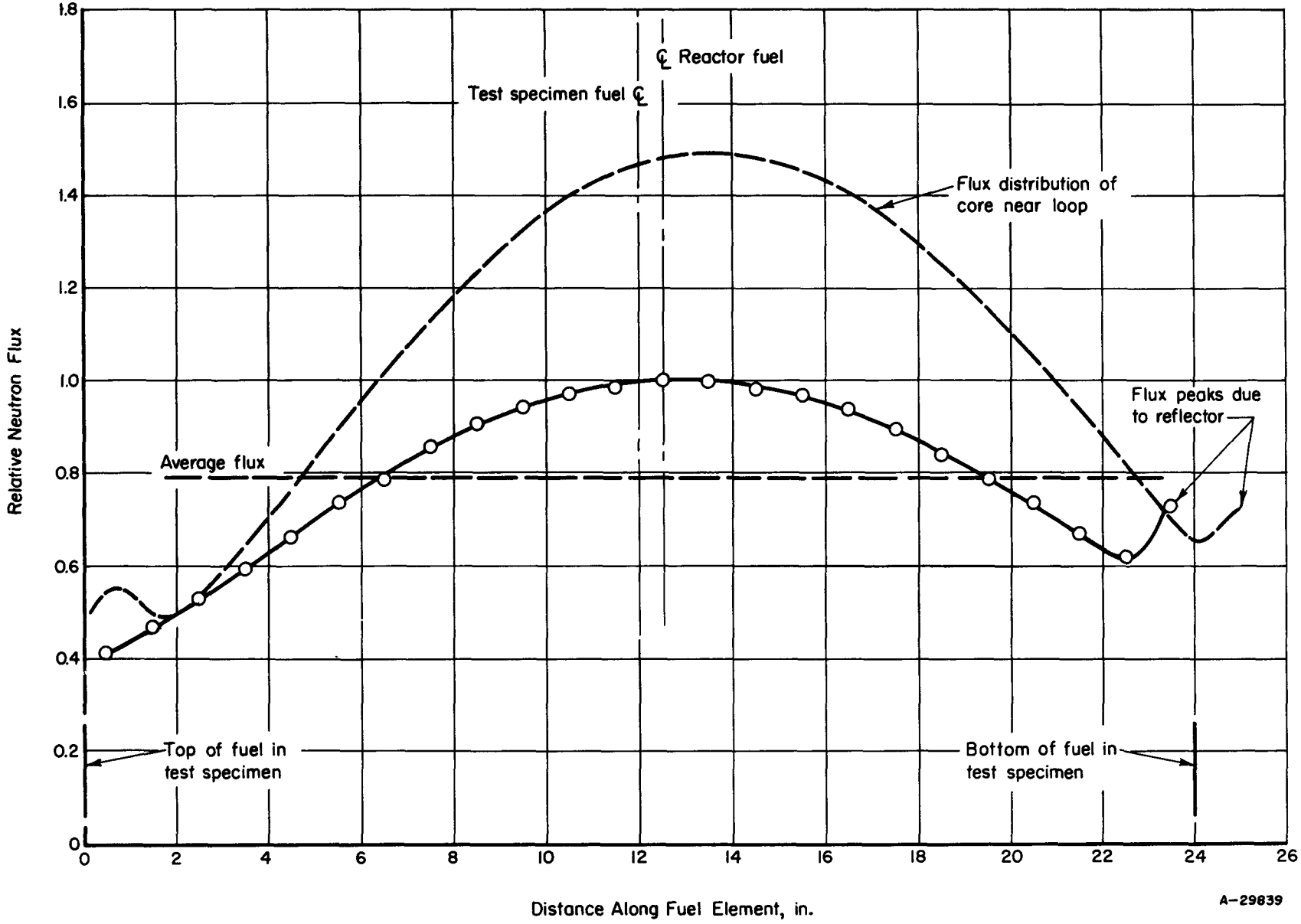

FIGURE 6. VERTICAL FLUX DISTRIBUTION

Peripheral Flux Distribution

The second series of flux measurements consisted of mapping the flux distribution around the periphery of the fuel element.* Six manganese-iron wires were arranged at 60-deg intervals around the periphery of the insulating sleeve of the element. The average peripheral variation of the flux obtained from the wire activities is shown in Figure 7. The angular variation was nearly independent of vertical location as indicated by the fact that the standard deviation of the data was only about ±3 per cent from the value plotted on the graph, i.e., the relative peripheral variation at each horizontal cross section was approximately the same. The curve shown in the figure is a cosine given by the empirical formula

$$\phi(\theta) = C \left[1 + 0.103 \cos \left(\theta - \frac{2\pi}{9} \right) \right], \qquad (2)$$

where C is a constant and θ is the counterclockwise angle from the normal to the core face. As seen from these data, the maximum flux occurs about 40 deg from the normal and the minimum is just opposite this location. The peripheral peak-to-average flux ratio is only 1.103, indicating approximately a 20 per cent flux decrease from the front to the rear of the element along the radius at 40 deg. The cosine behavior indicates a linear flux drop across the element. This gradient from roughly the center of the core out into the pool is to be expected and was indicated by the unperturbed flux measurements.

The radial flux plots were made at θ = 353 deg, where it was found that the radial depression from the outer fuel cylinder to the center of the element was a factor of 2.20. With the observed peripheral variation it is estimated that the maximum radial depression (occurring at θ = 40 deg) is 2.36 and the average depression is 2.14.

POWER PREDICTED FROM FLUX MEASUREMENTS

The flux distributions obtained from the wire activities were normalized to absolute thermal neutron flux by the gold-foil activation (corrected for epicadmium activation) at the front of the element at the horizontal center line. The thermal-neutron flux at this location was 3.70×10^{12} n/(cm^2)(sec). Since the fluxes were measured at the outer surface of the fuel cylinders, a depression factor must be included in the calculations to relate the surface flux to the average flux in the fuel. Assuming that the radial flux depressions indicated in Figure 5 are representative, the depression factor was obtained by assuming exponential attentuation between the end points of the flux in each fuel cylinder with no drop across the gas coolant channels.

*The fuel element used for these measurements was a twin to that used for the radial and vertical distributions.

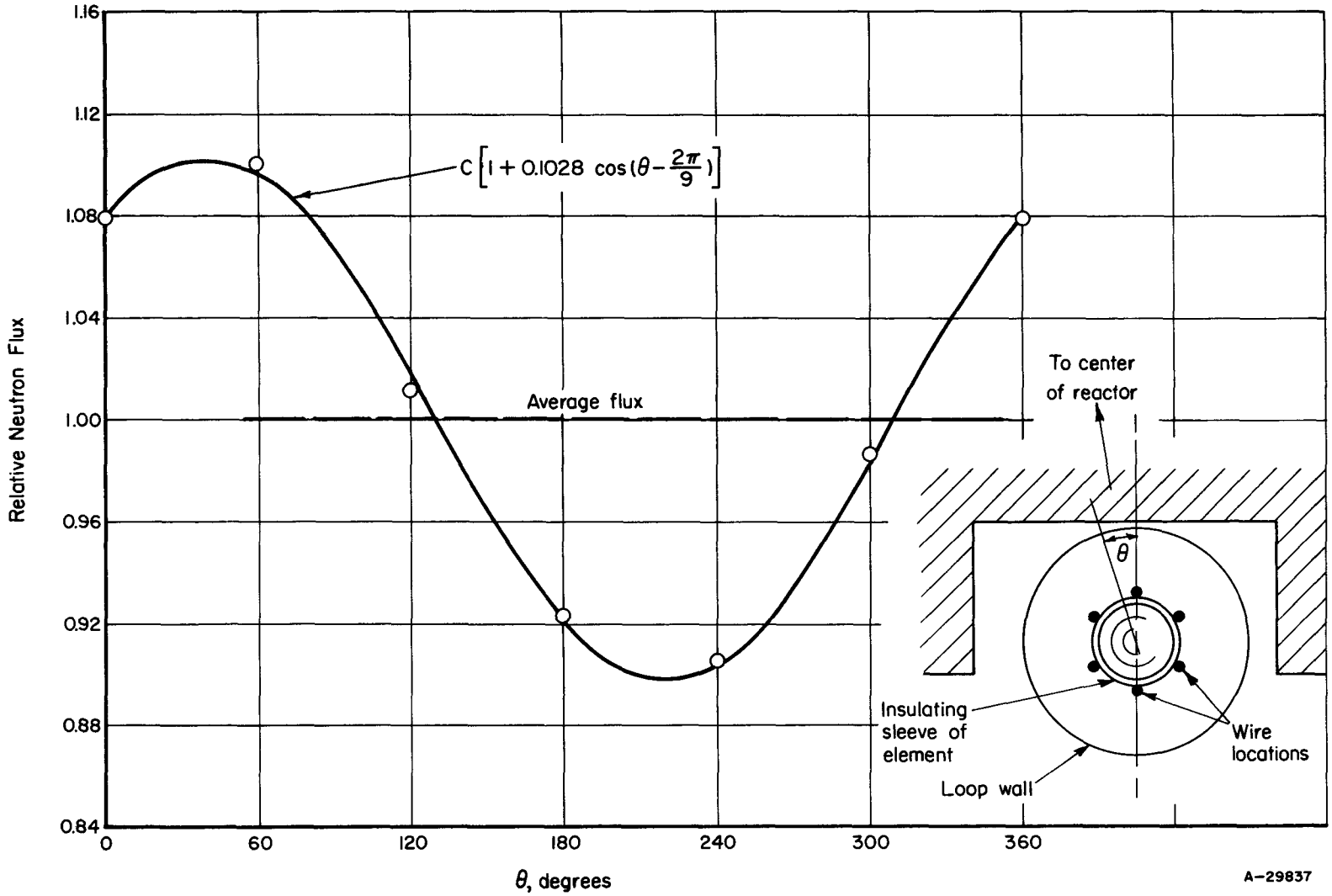

FIGURE 7. PERIPHERAL VARIATION OF NEUTRON FLUX

The power generated in each fuel cylinder due to thermal-neutron fissioning is

$$P_i = \overline{\phi}_{s_i} k_i m_i \left(\frac{E N_o \sigma_f}{A_U} \right), \tag{3}$$

where

P_i = power generated in the ith fuel cylinder due to thermal-neutron fissioning, w

$\overline{\phi}_{s_i}$ = average thermal-neutron flux at the outer surface of the ith fuel cylinder (averaged axially and around the periphery), $n/(cm^2)(sec)$

k_i = ratio of the average flux in the interior of the ith fuel cylinder to the surface flux of that cylinder

m_i = mass of uranium-235 in the ith fuel cylinder, g

E = sensible heat energy per fission in the element, w-sec per fission

N_o = Avogadro's number, 6.02×10^{23} atoms per g-mole

σ_f = microscopic fission cross section, $(584 \pm 10) \times 10^{-24}$ cm^2 per atom[6]

A_U = atomic weight of uranium-235, 235.1 g per g-mole.

A value of 180 mev per fission (2.86×10^{-11} w-sec per fission) has been estimated as the energy absorbed in the element per fission. This value includes 5.5 mev for gamma absorption, 0.5 mev for neutrons, and 9 mev for betas. Using these values and the measured fluxes, the power was calculated for each fuel cylinder. The calculations are summarized in Table 2.

TABLE 2. POWER GENERATED IN THE MARK II FUEL CYLINDERS DUE TO THERMAL-NEUTRON FISSIONING

Cylinder	m_i, g	$\overline{\phi}_{s_i}$, $n/(cm^2)(sec)$	k_i	P_i, w
1	26.72	1.15×10^{12}	0.985	1,290
2	41.12	1.31×10^{12}	0.944	2,180
3	54.38	1.77×10^{12}	0.863	3,560
4	70.13	2.46×10^{12}	0.850	6,280
			Total	13,310

Power Generated by Epicadmium Neutrons

The power generated in the fuel element by neutrons with energies above the cadmium cutoff energy (approximately 0.4 ev) was estimated from the measured gold-foil cadmium ratio of 2.48 at the front of the element (0-deg angular orientation). Assuming that the cadmium ratio does not vary significantly throughout the element and that the epicadmium flux has a 1/E distribution, the ratio, R, of epicadmium-to-thermal power is

$$R = \left(\frac{\sigma_{act}}{\sigma_f}\right)\left(\frac{\int \sigma_f \frac{dE}{E}}{\int \sigma_{act} \frac{dE}{E}}\right)\left(\frac{1}{CR - 1}\right), \qquad (4)$$

where

σ_{act} = microscopic thermal activation cross section for gold, 96×10^{-24} cm^2 per atom[6]

$\int \sigma_f \frac{dE}{E}$ = resonance fission integral for uranium-235, 271×10^{-24} cm^2 per atom[7]

$\int \sigma_{act} \frac{dE}{E}$ = resonance activation integral for gold, 1558×10^{-24} cm^2 per atom[8]

CR = cadmium ratio for gold.

With these values, R is 0.019 and thus the epicadmium power is only about 2 per cent of the thermal-neutron induced power. Since this contribution is small, little error is introduced in the total power by the assumption of constant cadmium ratio throughout the element.

With the above assumptions, the flux measurements predict a total power generation of approximately 13.6 kw. This indicates an average power density of 70.7 w per g of uranium-235. The ratio of peak power density in the element to the average power density was calculated from the flux distributions to be approximately 1.75.

DISCUSSION OF ERRORS

The errors associated with the measurement of the relative neutron-flux distributions are principally those incurred in counting and are generally small. As mentioned previously, corrections on the wire activities for axial variation of the cadmium ratio were found to be negligible. A small correction on the radial flux distributions is necessary due to radial variation of the manganese-iron cadmium ratio. Measurements through comparable thicknesses of fuel in a flat-plate element indicated a maximum

correction of 5 per cent in comparing the wire activities on the surface of the outer fuel cylinder with those at the center. This error probably represents the maximum error associated with the relative flux distributions. However, the error in the calculation of loop power due to this source is much smaller since the outer fuel cylinders predominate the power generation, as seen from Table 2.

The principal error in the measurements is associated with determining the absolute thermal-neutron flux. The estimated error in the thermal-neutron flux at the normalizing position was calculated from Equation (1) using a propagation of known errors in: (1) cesium standard activity, (2) microscopic activation cross section of gold-198, (3) detection efficiency of the counter, (4) cadmium ratio, and (5) experimental errors associated with the foil irradiation, including such items as positioning the gold foil in the mock-up, positioning the mock-up at the core face, correcting the indicated reactor power for instrument response to gamma rays, etc. The error contributed by Source (5) was estimated by examining the results of repeated gold-foil activations at several different reactor power levels, irradiation times, counting times, and decay periods, and the maximum deviation from the average value was found to be about 7 per cent. The total estimated error in the absolute flux determination is ±14 per cent.

Since the magnitude of error introduced by assumptions concerning the fine structure of the flux is not known, an estimate of the error associated with the power calculation is more qualitative. Assigning reasonable limits to the error in fine structure behavior and using the known deviations in the microscopic fission cross section, energy per fission, and absolute flux, the error associated with the calculated power is estimated to be about 20 to 25 per cent. The absolute flux determination is responsible for the largest portion of this estimated error.

COMPARISON OF FLUX-DETERMINED POWER WITH HEAT-BALANCE POWER

During loop operation the coolant-gas temperature increase across the test element and the gas flow rate are measured continuously, permitting a power determination independent of the flux measurements. The loop power obtained from the ΔT and flow-rate measurements does not include radial heat loss through the loop between the gas inlet and outlet. However, since the fuel cylinders are contained in an insulating sleeve (see Figures 2 and 4), this loss is estimated to be very small compared with the total loop power. Possible errors in determining the loop power by this heat-balance method indicate a precision of the order of 10 per cent.

It was observed during operation of the loop that the power level was affected by the position of the reactor control rods. During a reactor operating cycle*, three shim-safety control rods are moved incrementally from about 65 to 90 per cent withdrawn to compensate for xenon-poisoning effects, temperature changes, fuel depletion, etc. Under special conditions such as startup after an extended shutdown period or

*The reactor is operated continuously at full power for 12-day intervals separated by 2-day shutdown periods for maintenance and change of experiments.

startup at peak xenon shutdown poisoning, the control-rod positions may vary over even a wider range. The positions of the three-shim safety rods at any particular time during the cycle were averaged to obtain a gang position. The rods are generally kept evenly withdrawn and hence the gang position corresponds closely to the actual position of the rods. A correlation of loop power versus gang control-rod position based upon the data from several reactor cycles is shown in Figure 8. The scatter in the data is attributed to effects of regulating-rod movements, inaccuracies in the power measurements, and duplication of loop position at the start of each operating cycle. As seen from this correlation, the loop power varies from about 16 to 12.5 kw during a reactor cycle (rod positions ranging from 65 to 90 per cent withdrawn). Under special conditions loop powers up to 18 kw have been observed.

The flux measurements used to predict a power of 13.6 kw were made at a gang control-rod position of 91.0 per cent withdrawn. The loop power measured by heat balance at corresponding rod positions is 12.5 kw.

The agreement between the two methods is within 10 per cent and in general is better than would be expected, considering the many possible sources of significant error in calculating power from flux measurements. This agreement was obtained only after a large number of supporting experiments were performed and loop operation was well under way.

SUMMARY AND CONCLUSIONS

Flux measurements with the concentric-cylinder fuel element yielded data on the radial, vertical, and peripheral variations. To a good approximation it was found that these distributions were separable. The vertical flux distribution was cosine-shaped. The flux gradient from the reactor core out into the pool-water reflector caused a cosine peripheral variation around the loop wall. Characteristic properties of the flux and power distribution are summarized in Table 3.

TABLE 3. CHARACTERISTICS OF THE FLUX AND POWER DISTRIBUTION IN THE CONCENTRIC-CYLINDER FUEL ELEMENT

Item	Ratio of Peak-to-Average
Vertical flux distribution	1.26
Peripheral flux distribution[(a)]	1.10
Power density	1.75

(a) Measured around the periphery of the insulating sleeve.

The average radial flux depression from the surface of the outermost fuel cylinder to the center of the element was a factor of 2.14 and the maximum radial depression (occurring at θ = 40 deg) was approximately 2.36.

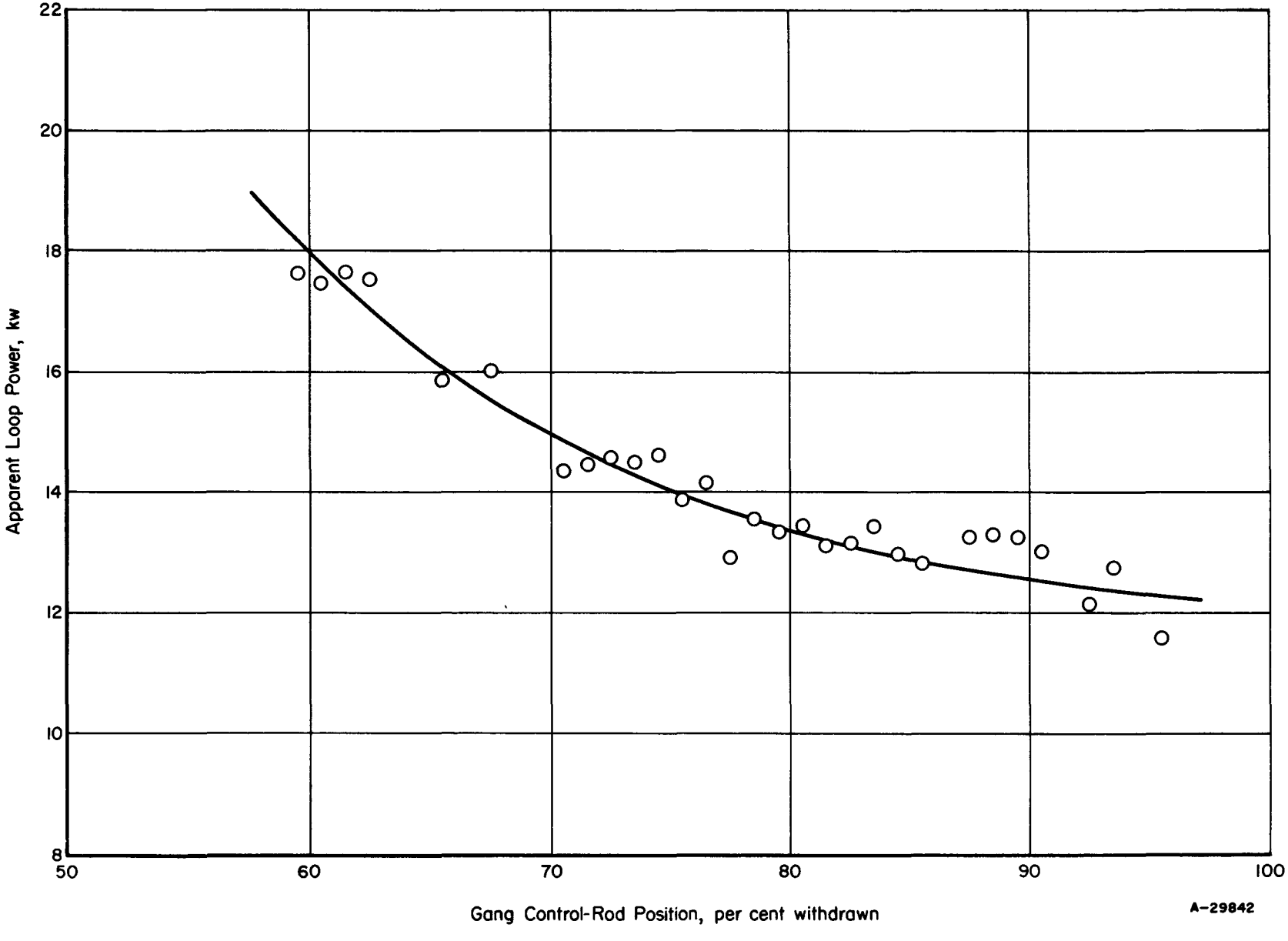

FIGURE 8. CORRELATION OF APPARENT LOOP POWER AND GANG CONTROL-ROD POSITION

The power predicted by the flux measurements agreed to within about 10 per cent of the loop power determined by measurement of the gas flow rate and ΔT across the test specimen. The error associated with the flux-determined power was rather large (20 to 25 per cent), due in part to the uncertainties in measuring the absolute thermal-neutron flux. The power generated by epicadmium neutrons fissions was about 2 per cent of the power due to thermal fissioning.

REFERENCES

(1) Bodnar, G. T., Stevens, W. J., Francis, G. A., Fawcett, S. L., and Rockwood, A. M., "An In-Pile Gas-Cooled Loop Installed at the Battelle Research Reactor", BMI-1290 (September 16, 1958).

(2) Morgan, W. R., Anno, J. N., and Chastain, J. W., Jr., "Neutron-Flux Measurements in a Flat-Plate Fuel Element", BMI-1231 (October 31, 1957). Confidential.

(3) Anno, J. N., Plummer, A. M., and Chastain, J. W., Jr., "Experience With a 1-Megawatt Pool Research Reactor", *Second International Conference on the Peacetime Uses of Atomic Energy*, P/422 (1958).

(4) Maienschein, F. C., Estabrook, G. M., Flynn, J. D., Johnson, E. B., and Henry, K. M., "Attenuation by Water of Radiations From a Swimming Pool Type Reactor", ORNL-1891 (September 7, 1955).

(5) Dingee, D. A., Ballowe, W. C., Klingensmith, R. W., Egen, R. A., Jankowski, F. J., and Chastain, J. W., Jr., "GCRE Critical-Assembly Studies", BMI-1288 (September 10, 1958). Confidential.

(6) Hughes, D. J., and Schwartz, R. B., "Neutron Cross Sections", BNL-325, Second Edition (July 1, 1958).

(7) Charpie, R. A., Horowitz, J., Hughes, D. J., and Littler, D. J. (Editors), Progress in Nuclear Energy, Series I, "Physics and Mathematics", McGraw-Hill Book Company, Inc., New York (1956), p 187.

(8) Davis, M. V., and Houser, D. T., "Thermal-Neutron Data for the Elements", Nucleonics, 16 (3), 89 (March, 1958).

JNA:BPF:JWC/ims